THE 5[TH] ASIAN COMPUTATIONAL FLUID DYNAMICS
BUSAN, KOREA, OCTOBER 27 ~ 30, 2003

DNS of Interaction Phenomena in Particle-Laden Turbulence

T. Kajishima
Department of Mechanical Engineering, Osaka University,
Yamadaoka, Suita, Osaka, 565-0871 Japan, kajisima@mech.eng.osaka-u.ac.jp

Abstract

A homogeneous flow field including more than 2000 spherical particles was directly simulated. Particles are settling by gravity with the Reynolds number ranging from 50 to 300, based on diameter and slip velocity. Particular attention was focused on the distribution of particles. The Reynolds-number dependence, influences of particle rotation and loading ratio, and the dynamics of particle clusters are discussed. In the higher Reynolds number case, the wake attraction causes particle clusters and the average drag coefficient decreases significantly. Non-rotating particles maintain cluster structure and rotating ones moves randomly in the horizontal direction. It is because of the difference in the direction of the lift force.

Keyword: *Direct Numerical Simulation, Two-phase Flow, Turbulent Flow, Vortex Shedding, Particle*

1. Numerical Method

The Cartesian coordinate system is selected for the DNS of particle-laden turbulence due to the following reasons[1,2]. The computational mesh, cubic in this study, does not fit the surface of spherical particles. The volume fraction of the particle in the cell, including solid-fluid interface, is taken into account [2]. The volume-weighted average of velocity $\boldsymbol{u} = \alpha \boldsymbol{u}_p + (1-\alpha)\boldsymbol{u}_f$ is introduced for two-way coupling between solid particles and fluid turbulence. α represents the volumetric fraction of the solid in the computational cell, $\boldsymbol{u}_f$ the fluid velocity, $\boldsymbol{u}_p (= \boldsymbol{v}_p + \omega_p \times \boldsymbol{r})$ the velocity in the solid body moving with velocity $\boldsymbol{v}_p$ and angular velocity ω_p. Based on the Navier-Stokes equation for $\boldsymbol{u}_f$, a governing equation for $\boldsymbol{u}$ is given as

$$\frac{\partial \boldsymbol{u}}{\partial t} = -\nabla \frac{p}{\rho_f} - \boldsymbol{u} \cdot \nabla \boldsymbol{u} + \nu_f \nabla^2 \boldsymbol{u} + \boldsymbol{f}_p . \tag{1}$$

The additional term, $\boldsymbol{f}_p = \alpha(\boldsymbol{u}_p - \hat{\boldsymbol{u}}_f)/\Delta t$ is given at the cell that includes the solid-fluid boundary. First, the unsteady equations for fluid flow are solved as if the field was occupied by fluid, and the result is denoted by $\hat{\boldsymbol{u}}_f$. Next, $\boldsymbol{f}_p$ modifies $\hat{\boldsymbol{u}}_f$ to $\boldsymbol{u}$ by $\boldsymbol{u} = \hat{\boldsymbol{u}}_f + \Delta t \boldsymbol{f}_p$. Thus, $\boldsymbol{f}_p$ is interpreted as the momentum exchange between the phases. The surface integral of the fluid stress τ in the equations for the particle can therefore be replaced by the volumetric integral of $\boldsymbol{f}_p$ as

$$\frac{d(m_p \boldsymbol{v}_p)}{dt} = \int_{V_p} \boldsymbol{f}_p dV + \boldsymbol{G}_p , \quad \frac{d(\boldsymbol{I}_p \cdot \omega_p)}{dt} = \int_{V_p} \boldsymbol{r} \times \boldsymbol{f}_p dV + \boldsymbol{N}_p . \tag{2}$$

where m_p denotes the mass of the particle, $\boldsymbol{I}_p$ the inertia tensor, S_p the surface, $\boldsymbol{n}$ the unit vector in the normal outward direction at the surface, and $\boldsymbol{r}$ the relative position from the center of rotation. The last two terms, $\boldsymbol{G}_p$ and $\boldsymbol{N}_p$, are external force and moment, respectively.

2. Results and Discussion

The periodic boundary condition is applied in all directions assuming the uniformity of the flow field. The computational cell is cubic. The number of them is $N_x = N_y = 512$ in horizontal directions and $N_z = 1024$ in vertical direction. The ratio of particle diameter to grid spacing is $D_p / \Delta = 10$, which allowed sufficient accuracy for vortex shedding at the particle Reynolds number range of interest [1, 2]. Figure 1 illustrates a computational domain and a part of instantaneous flow field obtained by such a setup. Four steps for the number of solid particles are calculated: $N_p = 256$, 512, 1024 and 2048. The corresponding loading-ratios are 0.05%, 0.1%, 0.2% and 0.4%, respectively. In such a relatively dilute loading, inter-particle collisions could occur, but are unlikely to dominate the particle distribution and the flow field. Thus, elastic collisions for simplicity are assumed in this study.

Initially, uniformly distributed particles and fluids are at rest. The density ratio between solid and fluid is $\rho_p/\rho_f = 8.8$. Hence, particles settle by gravity. To keep the mass flow rate of the mixture to zero, we adjusted the vertical gradient of pressure in the equation of fluid motion. The Reynolds number is adjusted as $Re_{ps} = 50$, 100, 200 and 300 by changing the fluid viscosity so that the gravity and drag are in balance.

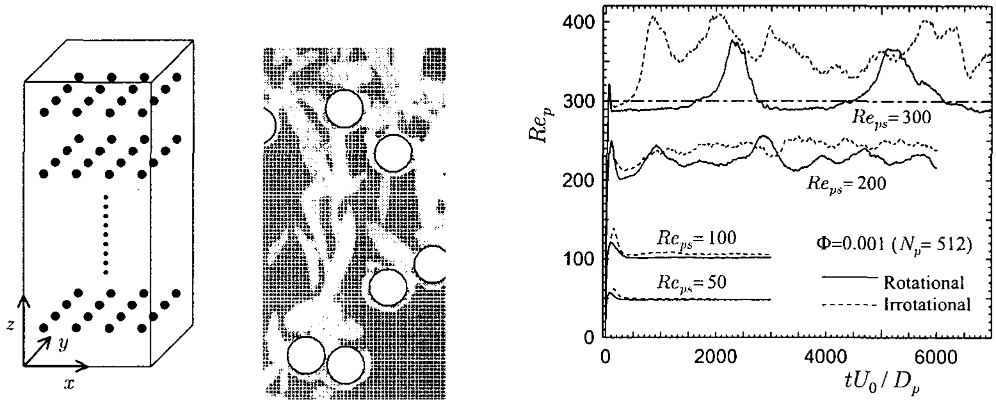

Fig. 1. Computational domain and initial condition (left), an example of instantaneous flow field caused by shed vortices (center) and time evolution of settling velocity ($\Phi = 0.001$, right)

3.1 Reynolds number dependence (Φ=0.1%) [3]

Figure 1 shows the time evolutions of averaged Reynolds number Re_p of settling particles. As for the lower Reynolds number particles Re_{ps} = 50 and 100, they fall with almost same velocity as a single particle does ($Re_p \approx Re_{ps}$) as shown in Fig. 1. The influence of particle rotation is insignificant. The inter-particle distances are therefore almost constant in these cases. TFor the intermediate Reynolds number $Re_{ps} = 200$, particles show collective behavior. Accordingly, the settling velocity becomes higher than that of a single particle of the same property, $Re_p > Re_{ps}$, as shown in Fig.1. For particles with higher Reynolds number, $Re_{ps} = 300$, vortex shedding takes place from each particle as shown in Fig. 1. In this case, the above-mentioned tendency becomes more evident. Moreover, the influence of rotation causes qualitative difference in collective motion of particles. The falling velocity becomes larger when particles form clusters. In this paper, the high-density region of particles is denoted by 'cluster'. The drag on a particle trapped into the wake of the other becomes smaller and it reaches to the other. Such a 'wake-attraction' is the mechanism of clustering in our case. Since many particles have less drag in the cluster, the average Reynolds number increases.

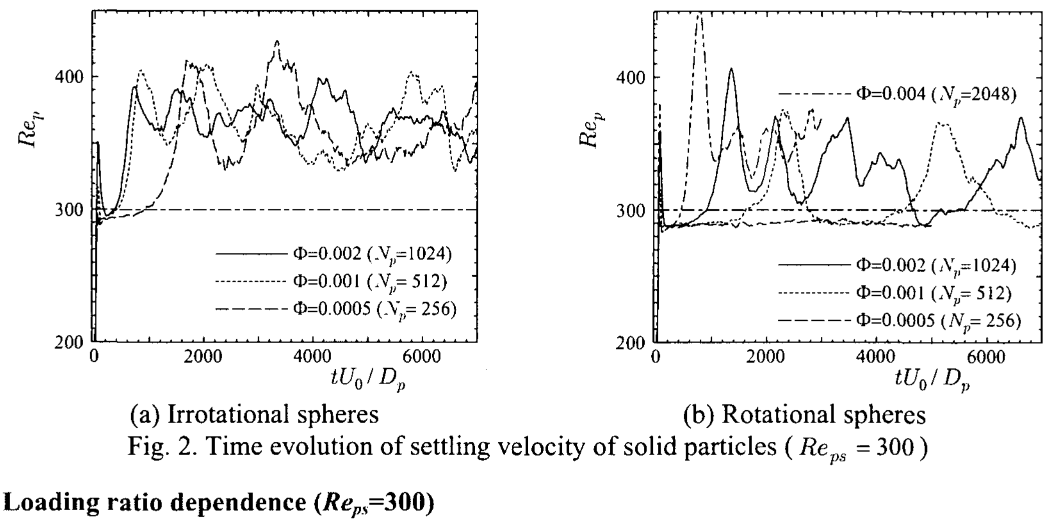

(a) Irrotational spheres (b) Rotational spheres

Fig. 2. Time evolution of settling velocity of solid particles ($Re_{ps} = 300$)

3.2 Loading ratio dependence (Re_{ps}=300)

Figure 2 compares the time evolution of averaged Reynolds number for irrotational and rotational particles of $Re_{ps} = 300$. Settling velocity of irrotational particles is faster than single particle by approximately 20%, regardless of the loading ratio. The behavior of actual particles, on the other hand, is affected by the mean loading ratio. For 0.05% volume loading, falling velocity of particles becomes lower than a sphere. In this case, particles do not form clusters. Thus the drag increases because they move independently in the self-induced turbulence. As the loading ratio increases from 0.1% to 0.2%, clusters are formed intermittently. Furthermore, for 0.4% loading, the number of clusters increases.

The particle rotation (figure omitted) increases during or slightly after the clustering, which is suggested by the increase in settling Reynolds number. It is probably because particle in the high shear region around clusters obtain the angular momentum. At the same time, the horizontal motion becomes larger due to the Magnus lift force (in horizontal directions). Once the motion perpendicular to the main velocity takes place, the orientation of vortex shedding tends to be fixed. Then the rotation and sliding motion are likely to be maintained due to the effect of inertia. This process is included in mechanism of break-up of clusters for rotational particles.

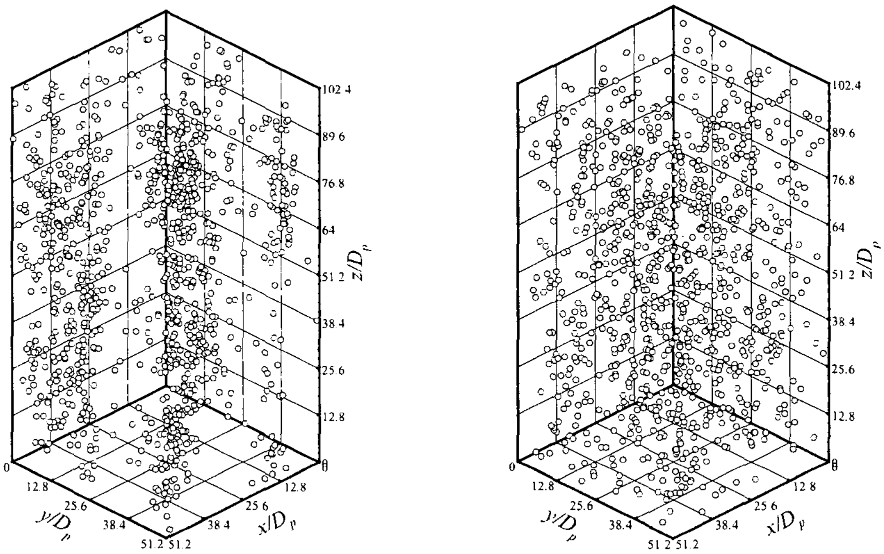

(a) Irrotational particles $(t = 3000D_p/U)$ (b) Rotational particles $(t = 5000D_p/U)$

Fig. 3. Instantaneous distribution of 1024 particles $(Re_{ps} = 300, \Phi = 0.002)$

3.3 Instantaneous distribution of particles (Re_{ps}=300, Φ=0.2%)

Figure 6 shows the instantaneous distributions of particles for 0.2% loading at the developed stage to compare the effect of particle rotation. Vertically elongated clusters are observed in Fig. 3(a). Particles trapped in these high concentration regions fall faster than average. By the movie, one can observe irrotational particles that once drop out from a cluster return to it or go into another cluster. Clusters behave somewhat dynamically but the structure is maintained. When the particle rotation is accounted for, firstly developed clusters have similar size and strength with those by irrotational ones. But the break-up is more complete. At the next step, regenerated clusters become larger but the particle density is lower. During the iteration of this process, the particle rotation grows as shown in Fig. 3(a). Consequently, the high concentration clusters such as initial ones are never reproduced as shown in Fig. 3(b).

References

[1] Takiguchi, S., Kajishima, T. and Miyake, Y., *JSME Int. J., Ser.B*, Vol.42, No.3 (1999) pp.411-418, 1999.

[2] Kajishima, T., Takiguchi, S., Hamasaki H. and Miyake, Y., *JSME Int. J., Ser.B*, Vol.44, No.4 (2001) pp.526-535.

[3] Kajishima, T. and Takiguchi, S., *Int. J. Heat and Fluid Flow*, Vol.23, pp.639-646, 2002.